Nano Today 55 (2024) 102217

Contents lists available at ScienceDirect

Nano Today

journal homepage: www.elsevier.com/locate/nanotoday

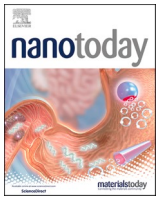

In-flight electro-neutralisation electrospray for pulmonary drug delivery

Hoai-Duc Vu [a,*], Trung-Hieu Vu [a], Ngoc Luan Mai [a], Deeptee Chandrashekhar Pande [b], Dzung Viet Dao [a], Bernd H.A. Rehm [b,c], Nam-Trung Nguyen [d], Gary D. Grant [e], Canh-Dung Tran [f], Yong Zhu [a], Van Thanh Dau [a,*]

[a] School of Engineering and Built Environment, Griffith University, Gold Coast, QLD 4215, Australia
[b] Centre for Cell Factories and Biopolymers, Griffith Institute for Drug Discovery, Griffith University, Nathan, QLD 4111, Australia
[c] Menzies Health Institute Queensland, Griffith University, Gold Coast, QLD 4222, Australia
[d] Queensland Micro and Nanotechnology Centre, Griffith University, Brisbane, QLD 4111, Australia
[e] School of Pharmacy and Medical Sciences, Griffith University, Gold Coast, QLD 4222, Australia
[f] School of Mechanical and Electrical Engineering, University of Southern Queensland, Toowoomba, QLD 4350, Australia

ARTICLE INFO

Keywords:
Electrospray
Drug delivery
Polymeric particles
Charge reduction
Micro/nanoparticles

ABSTRACT

Pulmonary drug delivery does not only provide non-invasive therapy for local lung diseases but also remarkably enhances systemic absorption of therapeutics owing to the tremendous surface area of the lung and fast transport of active molecules across the respiratory epithelia. In comparison to traditional delivery systems, electrohydrodynamic atomisation (EHDA) is superior in terms of size and production rate control but the high surface charges of resulting particles prohibit its use in drug delivery. To overcome this challenge, we developed an in-flight electro-neutralisation electrospray (IFENE) method which enables the generation of mists of particles in respirable size range with little to no charge. Our approach uses low-frequency alternating current (AC) to produce charge-neutralised sprays with initial velocity due to oppositely charged droplets combination. Experiments and simulations with pure liquid as the working solution were conducted to reveal the underlying mechanism. The applied frequency is found to be the main factor that influences spray stability and formation. Poly (vinylidene fluoride) (PVDF) and PVDF with curcumin solution were electrosprayed via IFENE, producing sprays of organic particles with controlled sizes and neutralised charges. The capability of coupling particle generation in the respirable size range (below 5 μm) and charge reduction (under 400 femtoamperes), along with its simple setup makes IFENE a promising platform technology in inhalation drug delivery.

Introduction

Advances in particle engineering technology have led to the rapid development of the design, synthesis, and application of inhalable micro/nanoparticles encapsulating therapeutics [1]. Micro/-nanoparticles were developed to improve the bioavailability of poorly water-soluble therapeutic(s), enhance cellular internalization, and facilitate sustained/targeted release of the loaded therapeutic(s) [2]. Inhalation of particulate therapeutics through oral or nasal administration routes represents a non-invasive delivery approach resulting in local or systemic application. Compared to oral and parenteral drug delivery, pulmonary drug delivery via inhalation offers significant advantages: (i) high drug absorption efficiency due to the large absorptive surface area of lungs (70–140 m^2) and thin epithelial layers (0.7–1.2 mm); (ii) avoidance of first-pass hepatic metabolism and acidic/enzymatic degradation in gastrointestinal tracts, thus allowing for high efficacy-to-safety ratio of therapeutic doses; and (iii) high blood flow in lungs facilitating systemic delivery [3]. Therefore, the development of pulmonary drug delivery has been directed toward the prevention or treatment of respiratory-based bacterial infections (e.g., tuberculosis, pneumonia, cystic fibrosis), viral infections (e.g., influenza, anthrax, respiratory syncytial virus), and non-infectious diseases (e.g., lung cancer, asthma), as well as for the systemic delivery of insulin or glucagon against diabetes [4].

In general, the development of micro/nanoparticles for pulmonary drug delivery involves two consecutive steps: (i) the production of particles loaded with therapeutics, and (ii) the aerosolisation of the particulate therapeutics. The deposition of particulate therapeutics in respiratory systems is determined by their aerodynamic diameters. Particles with aerodynamic diameters of above 5 μm accumulate

* Corresponding authors.
E-mail addresses: duc.vu2@griffithuni.edu.au (H.-D. Vu), v.dau@griffith.edu.au (V.T. Dau).

https://doi.org/10.1016/j.nantod.2024.102217
Received 5 September 2023; Received in revised form 1 February 2024; Accepted 22 February 2024
Available online 27 February 2024

preferentially in the upper respiratory tract (mouth, nose) [5–7]. Particles with aerodynamic diameters under 5 μm undergo deposition through three mechanisms: impaction, sedimentation, and diffusion. Impaction and gravitational sedimentation play crucial roles in deposition on the airway surface and within the smaller bronchi, respectively. Diffusion is the primary mechanism for particles of < 0.5 μm to be deposited in smaller airways and alveoli. [8–11]. Another factor that greatly influences the delivery ability of inhaled drug particles is their surface charge [12]. Particles with negative or neutral charges have more chance to go through the pulmonary air-blood barrier since the mucus has negative charges, which entraps positively charged particles [13,14]. Therefore, a technology that is simple but capable of controlling particle size and charge is ultimately desired, as it allows precise deposition of the particles in specific regions within the lung, thereby improving delivery efficiency, reducing drug exposure to non-targeted regions of the airway, and alleviating any harmful side effects [15].

Electro-hydrodynamic atomisation (EHDA) or electrospray is a preferred approach to generate micro/nanoscale particles for inhalable drug delivery as it is configurable to even encapsulate complex therapeutic molecules within a single droplet. Some noteworthy structures that can be fabricated via electrospray are core-shell [16–18], multi-layer core-shell [19], Janus particles [20], and multilobe particles [21]. This technique has been emerging as a powerful approach for drug discovery research [22–24] and is currently attracting research into the development of respiratory treatments including the generation and delivery of micro/nanoparticles as carriers for nano-medicine [25–27]. One fundamental drawback preventing EHDA itself from becoming a reliable dosing delivery system is that the generated droplets carry substantial surface charges. This is a significant factor that influences pulmonary drug delivery, as it promotes the adhesion of particles to unwanted areas along the delivery route [12]. The current technique using EHDA for drug delivery is (i) particle generation first then followed by (ii) particle delivery via inhalation devices such as nebulisers, dry powder inhalers, pressurised metered dose inhalers, or soft-mist inhalers (Fig. 1 A). To combine particle generation and delivery via inhalation in a single device for inhalable drug delivery or health care applications, the residual charge of particles must be reduced to weaken the electrostatic force in the inter-electrode space so that the particles can be conveyed out of the effect of reference electrode [28,29]. This process has attracted extensive research; for instance, by mixing the sprayed particle with oppositely charged droplets or oppositely charged gaseous ions [30–33], by using high-frequency alternating EHDA to stimulate a resonating meniscus at the orifice [34–36], by using low-frequency EHDA to self-neutralise droplet by matching their momentum with the alternating reversed electric field [37], or by using propelling ionic wind [38,39]. Nevertheless, most research efforts remained at the conceptual stage, neglecting in-depth investigation of the possibility to atomise biomaterials to serve as drug delivery carrier systems.

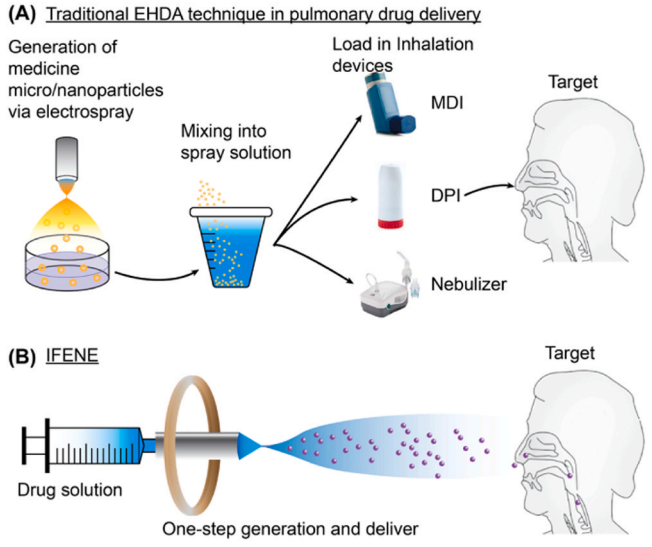

Fig. 1. (A) Traditional technique utilising electrohydrodynamic atomization (EHDA) in a multi-step drug delivery process. (B) In-flight electro-neutralisation electrospray (IFENE) provides one-step particle generation and delivery.

Here, we introduce the in-flight electro-neutralisation electrospray (IFENE) method, a novel platform that facilitates the generation of airborne particles with minimal to no charge, creating possibilities for one-step drug delivery (Fig. 1B). In this study, we (i) discussed the conceptual design and fundamental principles that underlie IFENE, (ii) examined the aerosolising ability of IFENE including spray stability and spray development, (iii) demonstrated IFENE's capacity to serve as a delivery platform for polymeric and drug-loaded particles into open space.

Results and discussion

Conceptual design

The AC electrospray configuration was first introduced in our previous work [37] without in-depth physics investigation and demonstration for potential application. In IFENE, solutions are atomised and delivered forward by an electrospray configuration shown in Fig. 2A (the detailed setup with electrical connection is shown in Figure. S1). By putting the counter electrode i.e., the metal ring, at a distance behind the tip of the nozzle, the electric field at the meniscus is warped back into the ring, subjecting the emitted charged droplets to decelerate and eventually moving back to the ring as shown in the electric vector field and experimental images in Fig. 2B. In IFENE, to create a neutralisation effect, alternating current (AC) at sub-kilohertz is applied to the system to create periodic sprays of oppositely charged droplets. When the charged droplets from an AC half-cycle are still in close proximity to the nozzle and being slowed down by the backward electric field, they accelerate the droplets of the next AC half-cycle (with opposite charge) through electrostatic force. Consequently, the succeeding droplets can catch up, allowing for mixing. This mixing process instantaneously neutralises or substantially reduces the charges carried by the droplets. The electro-neutralised droplets continue their forward movement due to the retained momentum, while the electric field has no effect on them. The plume of charge-reduced aerosol generated by IFENE can be observed in Fig. 2A.

The key physical mechanisms to neutralise charged aerosol of IFENE are droplet catch-up and oppositely charged droplet mixing. A numerical model with simulation employing both fluid flow and electrostatic physics is utilised to confirm the mechanism. The model uses Taylor-Melcher's leaky-dielectric model [40], commencing with the continuity and the momentum equations for the fluidic fields:

$$\frac{\partial \rho}{\partial t} + \nabla \cdot (\rho \boldsymbol{u}) = 0 \tag{1}$$

$$\rho \left[\frac{\partial \boldsymbol{u}}{\partial t} + (\boldsymbol{u} \cdot \nabla)\boldsymbol{u} \right] = -\nabla p + \eta \nabla^2 \boldsymbol{u} + \boldsymbol{f}_\sigma + \boldsymbol{f}_e + \rho \boldsymbol{g} \tag{2}$$

where ρ is the fluid density, t is the time, $\boldsymbol{u}$ is the fluid velocity, p is the pressure, η is the fluid viscosity, and $\boldsymbol{g}$ is the gravitational acceleration. The surface tension force $\boldsymbol{f}_\sigma$ and electrostatic force $\boldsymbol{f}_e$ arise to consider multiphase behaviours and electrostatic involvement. The surface tension force is calculated per unit volume by the continuum surface force (CSF) model [41]:

$$\boldsymbol{f}_\sigma = \sigma \kappa \nabla \gamma_{liq} = -\sigma \nabla \cdot \left(\frac{\nabla \gamma_{liq}}{|\nabla \gamma_{liq}|} \right) \nabla \gamma_{liq} \tag{3}$$

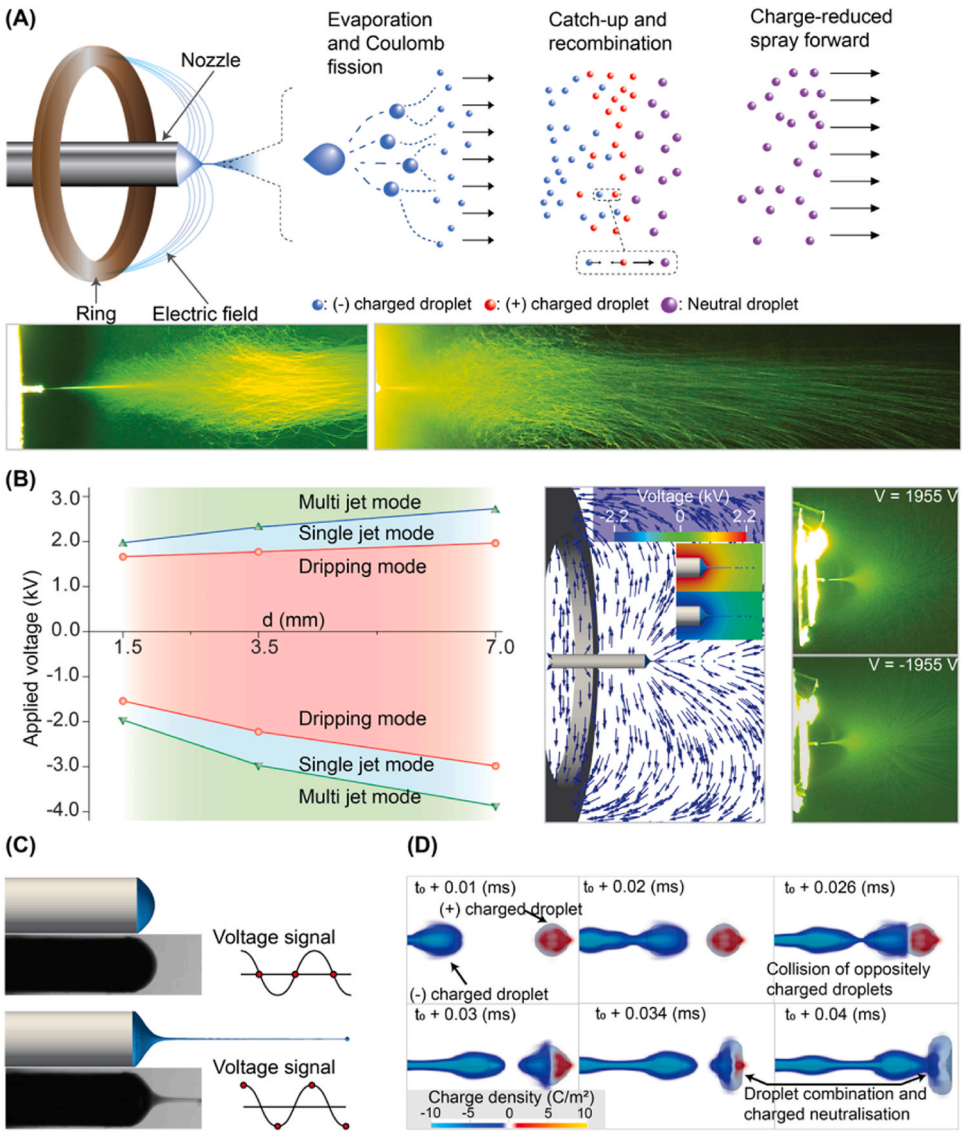

Fig. 2. Proposed concept. (A) Schematic and concept of in-flight electro-neutralisation electrospray (IFENE) with experimental images showing the spray formation (left: near field; right: far field). (B) The configuration working in DC mode: spray mode, numerical simulation, and experimental images of the spray in single-jet mode. (C) Simulation of the Taylor cone in AC mode compared with experimental captures. (D) Time sequence of the neutralising process in simulation.

with σ as the surface tension coefficient and κ as the mean curvature of the free surface. The phase fraction of liquid γ_{liq} is solved by the VOF method to capture the interface in the inhomogeneous fluid field [42] with an artificial compression term for higher interface resolution [43]. Fluid density and viscosity are defined via arithmetic averaging with the phase fraction.

Electrostatic governing equations are solved neglecting the magnetic induction estimate of the electrostatic force f_e, which initially involves Gauss's law $\nabla\cdot(\varepsilon \boldsymbol{E}) = \rho_e$ together with the relation $\boldsymbol{E} = -\nabla\phi(t)$, formulate Poisson's equation for electrostatics. Subsequently, the conservation of charge equation is considered. The electrical conductivity and the electrical permittivity are defined by harmonic averages throughout the computational domain [44]. Finally, the electrostatic force is the summation of the Coulombic force and polarisation force [45]:

$$f_e = \rho_e \boldsymbol{E} - \frac{1}{2}|\boldsymbol{E}|^2 \nabla\varepsilon \tag{4}$$

Details of numerical simulation are shown in Section S1 including full governing equations and simulation domains.

Fig. 2C depicts the outcomes of the simulation running under an applied AC voltage and the same operating conditions as the compared experiment, with a focus on the Taylor cone. The simulation is well-validated with experimental results concerning Taylor cone geometrical parameters (the cone half-angle and the jet diameter) and its transient state behaviour (detailed comparison is illustrated in Figure. S3). With a focus on the trajectory of the ejected droplets at a substantially large distance from the tip of the nozzle, Fig. 2D demonstrates the catch-up and combination process of two oppositely charged droplets. The resulting droplet's charge is neutralised, as the charge density is significantly reduced. With the momentum from the preceding droplet, the combined droplet keeps moving forward as the process repeats. The duration of the neutralisation process is larger than the period of a half-AC cycle, i.e., the time for one spray of charged droplets, thus leading to an incomplete neutralisation of all electrosprayed droplets. While the simulation confirms the neutralisation process through a simple collision model, it falls short in incorporating all physical phenomena happening in the mixing zone. These include evaporation [46], coalescence and breakup of oppositely charged droplets [47,48], corona discharge [49] and collective behaviour of charged droplets.

Improvement on the numerical model would include considering more models that could capture the physical processes and optimising to achieve synchronisation between the combination rate and charged particle production frequency.

Spray stability and formation

The investigation into spray stability uses isopropyl alcohol (IPA) as the working liquid, a pure fluid of low surface tension, instead of surfactant solutions, with the intent to exclude surface tension gradients due to non-uniform distribution of surfactant molecules under a focused electric field. The Taylor cone of IPA liquid, which was recorded with a high-speed camera, reveals its transient behaviour. This behaviour which includes the emission of a jet and meniscus oscillation without liquid ejection is synchronised with the AC voltage signal, observed in both single-jet mode and multi-jet mode (Fig. 3B-C). Through high-speed capture, the stable state of the Taylor cone is deemed as the unchanged shape of the cone jet at every AC half-cycle. Investigation in operating parameters results in Fig. 3A, in which, IFENE with small interelectrode distance require lower voltage to activate steady single-jet mode. Fig. 3A also reveals the frequency effects on the required applied voltage. The bounded voltage for single-jet mode is lower as the frequency increases. However, at 1 kHz and higher, the system fails to generate a stable spray. The optimal range of frequency for power consumption is from 100 to 500 Hz.

Fig. 3D illustrates the dependence of the direction of the sprayed jet stream on the applied frequency. The direction of the spray is quantified by the spray angle θ, which is defined by the trajectory of the outermost particle observed in experiments. The applied voltage is adjusted to achieve the steady single-jet spray mode. At 10 Hz and lower, the sprayed particles travel back towards the ring, similar to the behaviour observed in DC mode. At increased frequency, θ drops quickly and at the frequency above 100 Hz, the jet stream shifts to a forward direction, maintaining a stable θ at approximately 10°.

Unlike the DC-driven mode, ions generated by AC driven regime tend to localise with the increase of the applied voltage frequency due to a

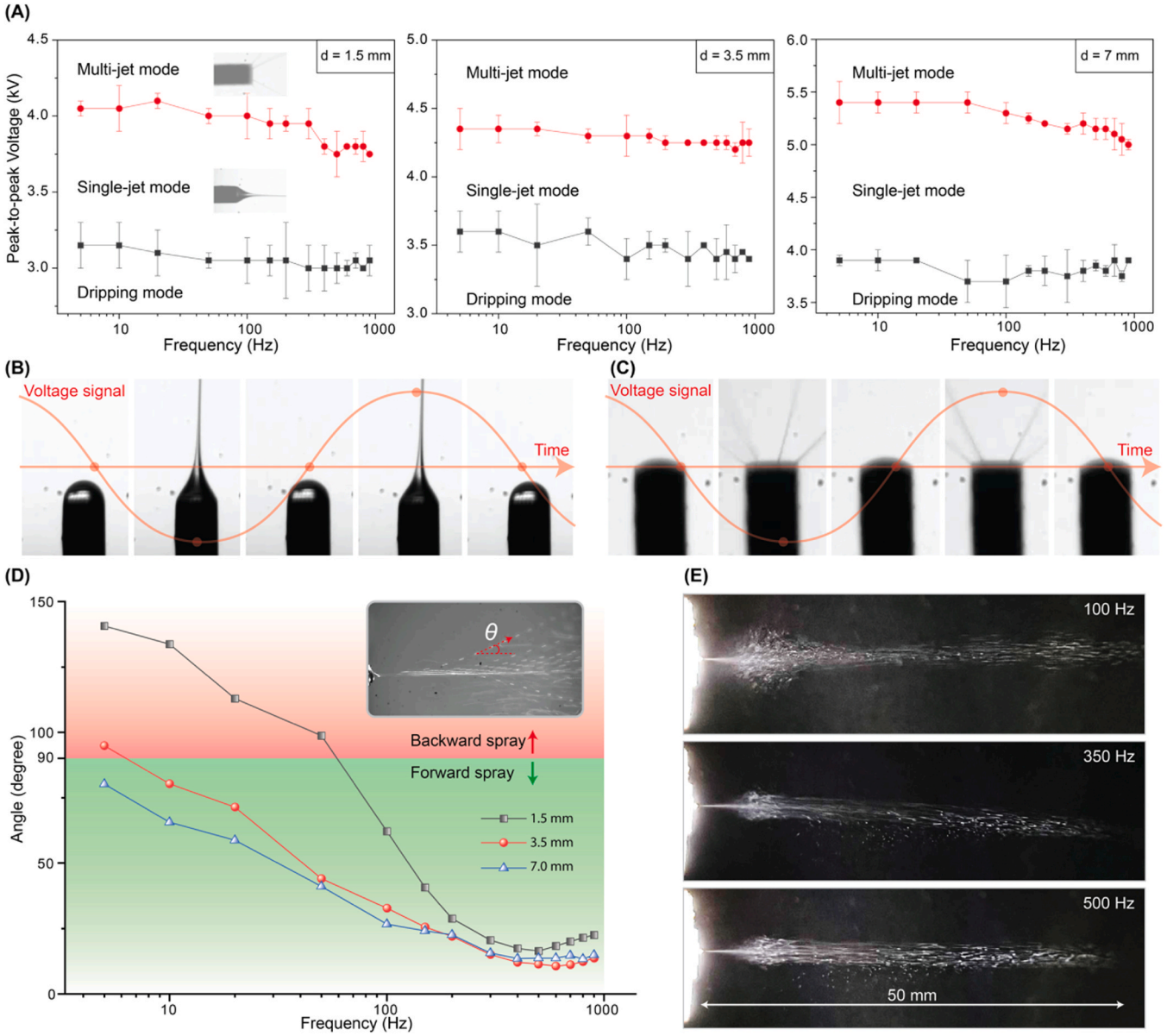

Fig. 3. Spray regime with Taylor cone capture. (A) The spray mode depends on applied voltage and frequency. (B) Taylor cone capture sequences of single-jet mode and (C) multi-jet mode in one AC cycle. Quantified spray direction and spray length. (D) Spray angle (θ) plotted versus the frequency ranging up to 1000 Hz for different interelectrode distances 1.5 mm, 3.5 mm, and 7 mm respectively. (E) Spray visible length in an enclosed environment at different frequencies.

recombination of ions occurring at the region close to the electrodes. For the IPA solution, the charge relaxation time $\beta\epsilon_0/K$ is estimated to be in the order of tens of microseconds which is much shorter than the switching time of the applied electric field. The optimal frequency is estimated from experimental Taylor cone dimensions (from high-speed camera capture in Figure. S3) to be in the range of several hundred hertz which agrees well with the experiment results of spray angle in Fig. 3D. In this range, the effect from space charged, and forwarding momentum of the sprayed droplets are dominant and the droplets do not reach the ring electrode. Instead, the droplets join in mixing with the oppositely charged ones. This mixing zone can be observed in Fig. 3E. From the mixing zone, the charged droplets not participating in neutralising process fly toward the ground electrode while the neutral aerosols travel in the forward direction. The wider spread-out of the mixing zone at 100 Hz indicates lower rate of combination, whereas at 500 Hz, the mixing zone is narrowed down, indicating a higher rate. These results agree with the spray angle results, making θ one of the reliable quantities to evaluate the effectiveness of IFENE.

Generating airborne organic particles via IFENE

Through in-flight neutralisation of droplet charges, IFENE facilitates generating sprays of particles made of multiple materials with low charges and initial velocity in one step, which makes it a potential device for pulmonary drug delivery. To validate this innovative approach, a polymeric solution i.e., polyvinylidene fluoride (PVDF) solution was

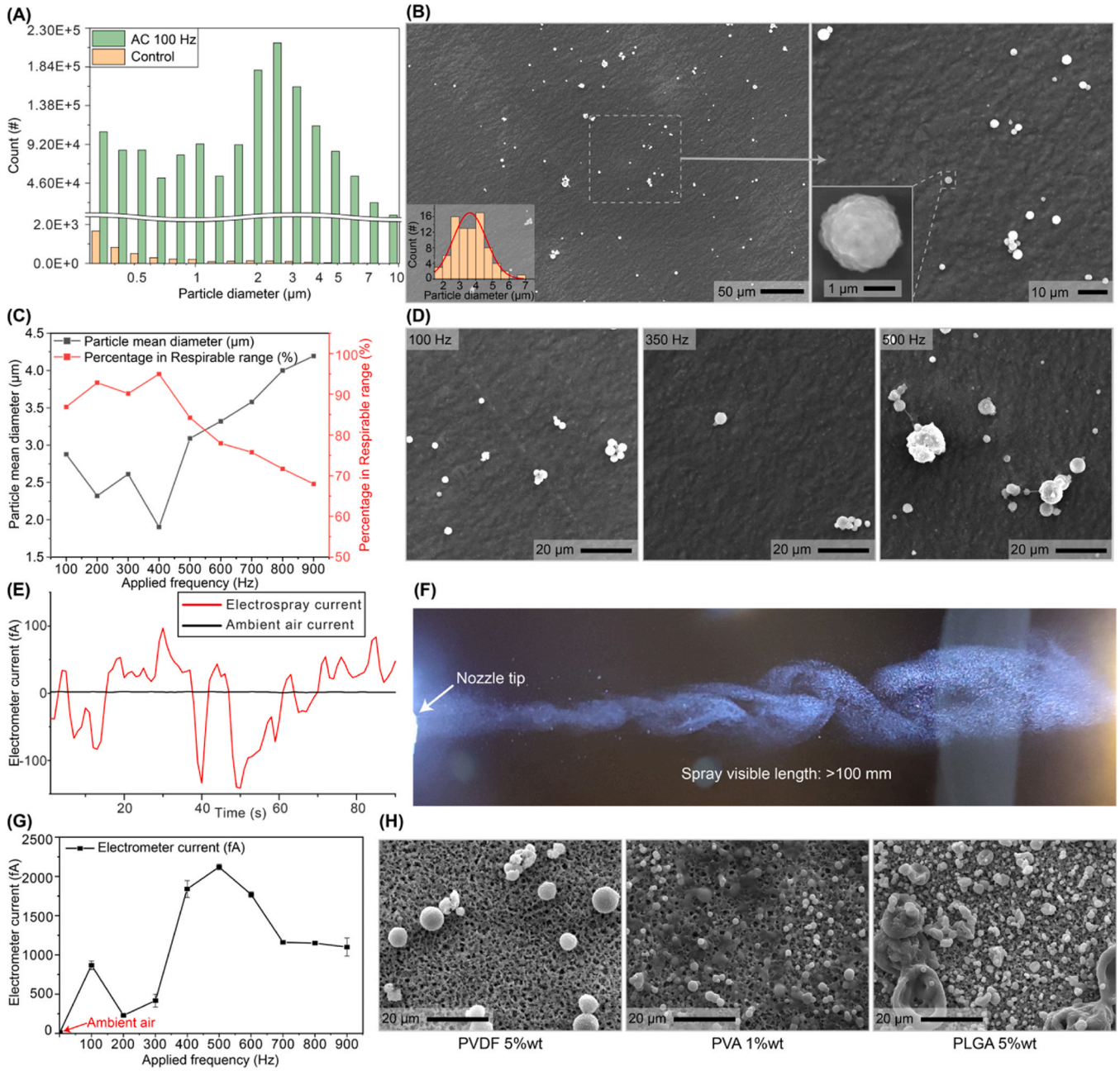

Fig. 4. Polymeric particles generation and characterisation. (A) – (G): PVDF particles. (A) Optical Particle Sizer (OPS) data of particle diameter for the operating frequency of 100 Hz. (B) SEM image of collected particles at the same operating conditions. (C) OPS data of particles mean diameter and percentage of particles in respirable range at different frequencies. (D) SEM images at three different frequencies: 100 Hz, 350 Hz, and 500 Hz. (E) Electrometer current of the spray. (F) Camera capture of the sprayed PVDF plume. (G) Average electrometer current of the spray at different frequencies. (H) SEM images of different types of polymer particles generated by IFENE.

employed in the IFENE system and the generated polymeric particles were characterised in aerosol form and particle-on-substrate form. The optical particle sizer (OPS) data in Fig. 4A shows aerodynamic diameters of in-flight particles with relatively small size distribution and a mean diameter of 2.87 μm. This size distribution also agrees with the SEM image analysis in Fig. 4B. In the SEM image, most of the PVDF particles are in spherical shape with uneven surfaces. In Fig. 4C, a substantial proportion of particles (70 – 95%) falls within the respirable range across different applied frequencies [50]. The particles mean diameter increases with the frequency surpassing 400 Hz while the percentage of particles in respirable size range decreases sharply. This trend is further shown in Figure S4 where a noticeable shift to higher diameters as frequency increases beyond 400 Hz can be observed in the size distribution. The increase in frequency also shows an increase in the number of particle clusters in the SEM images (Fig. 4D). This is due to the incomplete coalescence of smaller charged particles in the neutralisation process. A possible explanation for this observation is that with increased AC frequency, the rate of collision of oppositely charged droplets increases, leading to a greater number of droplets coalescing mid-air. When the solvent evaporates, the collected remains are clusters of PVDF particles. Nevertheless, the electrospray plume charge is proved to be substantially reduced as the particles collected into the electrometer have a current in the order of several hundred femtoamperes, as showcased in Fig. 4E. Fig. 4G presents the average charge level of the spray across various applied frequencies. At frequencies below 300 Hz, the charge level remains below 1 pA. With an increasing applied frequency, a surge in charge level can be observed, peaking around 2 pA. Beyond 700 Hz, the charge level stabilises at around 1.1 pA. The changes in charge level can also be explained by the different rates of collision of charged particles, as they are influenced by the applied frequency. From these values, IFENE could be considered to generate electro-neutral particles when compared to conventional inhalation drug delivery devices[51–55]. Detailed comparisons can be found in Section S2. While the respirable size and neutralized charge of IFENE particles imply a potentially high inhalation efficiency, additional studies of median mass aerodynamic diameter and aerosol outputs are necessary to address this observation quantitatively. Fig. 4F shows IFENE in operating with the plume of airborne PVDF particles flies forwards and can travel more than 10 cm. Video capture of the operation of IFENE in generating PVDF particles can be found in the movie S1.

Supplementary material related to this article can be found online at doi:10.1016/j.nantod.2024.102217.

In support of the potential of IFENE as a drug delivery platform, two alternative polymeric solutions, polyvinyl alcohol (PVA) and poly (lactic-co-glycolic acid) (PLGA), were investigated. Fig. 4H presents the SEM images of the particles generated by these polymeric solutions in comparison to PVDF solutions. While distinctive morphologies and size distributions can be observed within each type of polymeric particle, the spray process consistently achieves the desired properties in terms of size distribution and charge level for pulmonary drug delivery. These observations provide further validation for the potential applications of IFENE, though comprehensive investigations are required in the future to gain a better understanding of the electro-neutralisation process and the effects of solution parameters on the aerosols.

The ability to generate polymeric particles has particular relevance for drug delivery because polymers have been proven to be an effective carrier for drugs as they are easy to modify to achieve well-defined properties [56]. Building upon the findings obtained from atomising PVDF solutions, we investigated whether IFENE can be applied to incorporate curcumin into PVDF particles. Curcumin, a yellow pigment sourced from turmeric, has an extensive history of uses in culinary and medicinal practices spanning centuries. Beyond its traditional uses, curcumin finds diverse applications in biotechnology and health [57]. In the field of pulmonary diseases, curcumin has shown its potential in the treatment of asthma, pulmonary fibrosis, cystic fibrosis, lung injury, and lung cancer [58,59]. Prior research has highlighted the potential of curcumin-loaded micro/nanoparticles generated through the electrospray method. Electrospray serves to overcome limitations associated with curcumin delivery such as low solubility and poor bioavailability [60,61].

Upon delivery by IFENE, the PVDF-Curcumin aerosols show differences in size distribution measured by OPS in Fig. 5A as curcumin-incorporated particles diameter is mostly under 1 μm. SEM image in Fig. 5B gives a similar size distribution of the collected particles. Clusters of particles which are the results of incomplete combinations of particles were observed to have a high frequency of occurrence in the collected samples. To examine the ability of PVDF particles to carry the cargo, SEM-EDS (Energy Dispersive Spectroscopy) analysis was conducted to detect curcumin. In PVDF EDS mapping shown in Fig. 5C, the particles mostly carry traces of carbon and fluorine, which are the main elements in its chemical composition ($-(C_2H_2F_2)_n-$), while the PVDF particles loaded with curcumin have substantial traces of oxygen, which is in curcumin chemical composition ($C_{21}H_{20}O_6$). Focusing on specific particle points, the PVDF particles loaded with curcumin also show a higher intensity of oxygen spectrum peak. The electrosprayed PVDF-curcumin plume was analysed with the electrometer, showing an extremely low level of charge (Fig. 5D). In addition to particle size and surface charge, the assessment of loading capacity (LC) and encapsulation efficiency (EE) are important in evaluation of IFENE as a potential drug delivery platform. EE for PVDF-curcumin particles was found to be $89.5 \pm 2.1\%$ and LC to be $32.4 \pm 5.0\%$. Notably, high encapsulation efficiency was also reported in other drug delivery applications utilising electrospray technique [62–64]. The release kinetics of curcumin from PVDF-curcumin particles was studied for 72 hours (Fig. 5E) in PBS solution and continuous curcumin release was observed throughout this time. The first 12 h exhibited a rapid and approximately linear drug release profile, reaching 40.26%. Subsequently, a sustained release phase with reduced release rates was observed. After 72 h, 68.69% of the encapsulated curcumin was released. Finally, the visible spray in Fig. 5F can be observed to have a yellow colour contributed by curcumin (The video capture of the operation of IFENE in generating curcumin-incorporated particles could be found in the movie S2). These collective observations serve as compelling evidence, underscoring the successful incorporation of curcumin within the electrosprayed airborne particles and promising potential of the particles in sustained drug release.

Supplementary material related to this article can be found online at doi:10.1016/j.nantod.2024.102217.

Conclusions

Here, we presented IFENE, a method for generating extremely low-charged particles, which formation could be controlled by both spray mode and plume formation. IFENE is built upon the concept of low-frequency electrospray and in-flight oppositely charged particles mixing. This initial concept [37] and its underlying mechanism were confirmed by experiments and numerical simulation. The generation of low-charged plumes of micro/nanodroplets with a forward momentum by electrospray omits the need for a separate delivery device and simplifies the drug delivery process. Operating parameters tuning show that the spray mode and spray angle, which determine the formation of the plume of particles, are mainly influenced by the applied frequency. However, intensive experiments and numerical modelling are needed to further understand the physical phenomena behind the concepts.

IFENE was demonstrated to enable the production of multiple types of polymeric and organic-incorporated micro/nanoparticles. These particles generated via IFENE showed characteristics that could overcome physicochemical barriers of inhalable nanomaterials such as size and surface charges [12]. The diameters of particles are in the range of under 10 μm, with the majority in the respirable range below 5 μm, and can be controlled by tuning the combination rate through applied frequency. Remarkably, the particles possess an extremely minimal charge

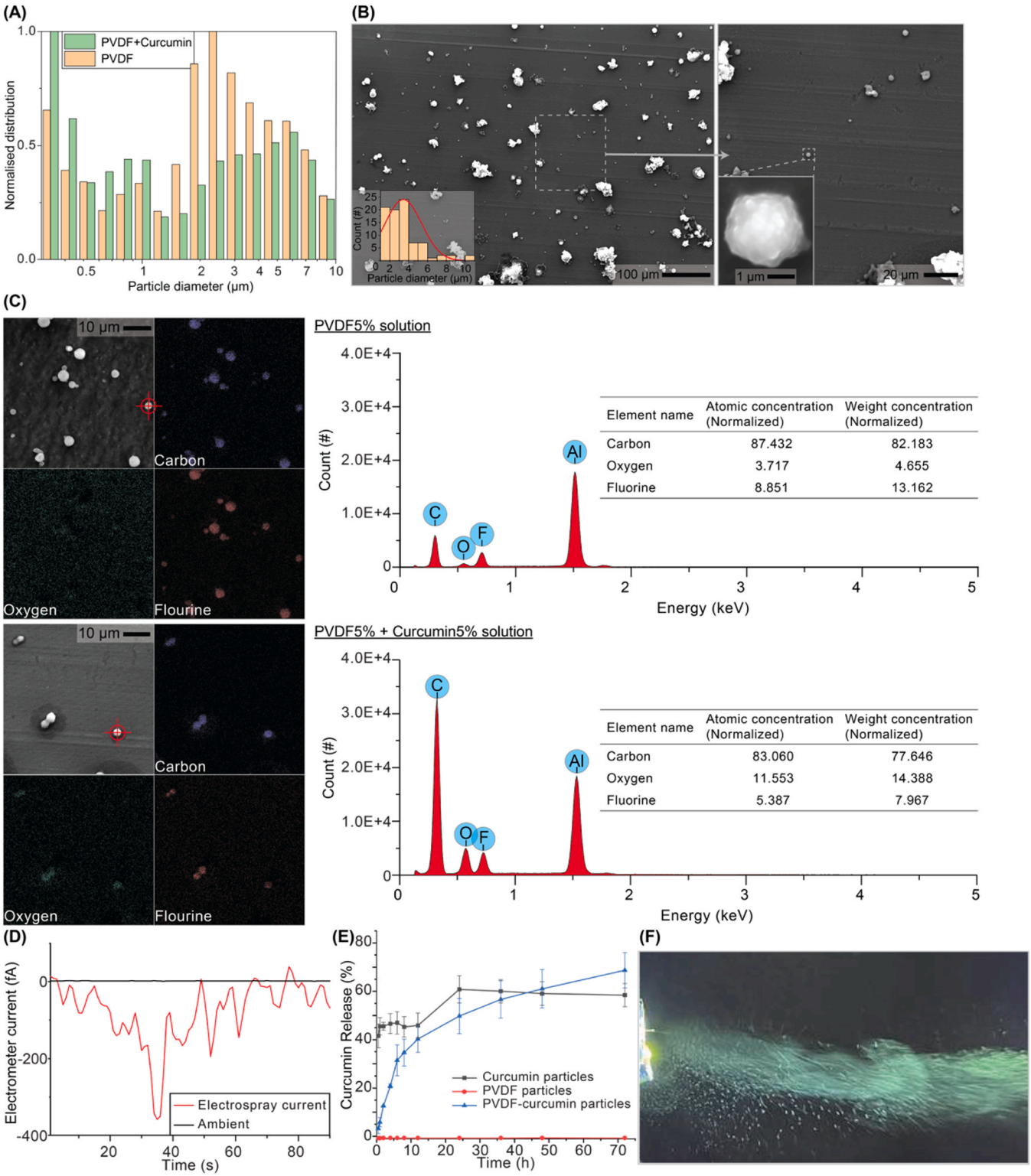

Fig. 5. Curcumin loaded PVDF particle generation and characterisation. (A) OPS comparison data of PVDF and PVDF-curcumin particles. (B) SEM images of PVDF-curcumin particles (C) SEM-EDS analysis (map and point) of the electrosprayed PVDF and PVDF-curcumin particles. (D) Electrometer current profile of PVDF-curcumin aerosol spray generated by IFENE system (E) Curcumin release profile of PVDF-curcumin particles (with comparison to curcumin and PVDF particles) (F) Visible plume of the electrosprayed PVDF-curcumin solution.

level (pico- to femto-ampere level). The results suggest a high inhalation efficiency for the platform. Nevertheless, further studies, including mass median aerodynamic diameter and aerosol outputs are planned in the future to quantitatively confirm this observation. Investigation into the curcumin incorporated particles revealed high encapsulation efficiency and reasonable loading capacity. The drug release kinetics profile of the generated particles indicated promising potential for sustained release. Finally, IFENE presents the ability to produce a plume of particles with forward momentum without any assisting propelling.

In future development, advanced techniques such as magneto-

electrospray or coaxial electrospray could be integrated into the IFENE system to facilitate generation of functional complex structure particles. This potential opens possibilities for IFENE to become a platform technology, not only in drug delivery applications but also in other fields such as environmental science and agriculture.

Materials and methods

Device preparation and spray investigations

The electrospray setup used a 30-gauge nozzle (Musashi Engineering) with outer and inner diameters are 0.312 mm and 0.159 mm, respectively. A metal ring with an inner diameter of 3.8 mm was located upward of the capillary tip and kept concentrically with the nozzle by a 3D-printed holder. The distance between the tip of the nozzle and the ring in the horizontal plane is called the interelectrode distance (d). The AC voltage was generated by a voltage amplifier (hivolt.de GmbH & Co. KG) connected to a signal generator (RIGOL). The high-voltage signal was connected to the nozzle and the ground wire was connected to the metal ring. To control the flow rate, a syringe pump (New Era pump systems Inc) and plastic syringe (1 ml) (Terumo) were used. The dynamics of the Taylor cone during the operation were continuously monitored and recorded with a high-speed camera (Mega Speed) with a speed up to 4000 fps and a microscopic lens (INFINITY). The plume was recorded with a digital microscope (Dino-lite EDGE™) and a normal camera. Experiments were conducted at room conditions (temperature 20 − 21°C). The experiment schematic is shown in Figure. S1.

The working liquid is isopropyl alcohol 99.5% (IPA) (Sigma-Aldrich), with surface tension of 20.8 mN/m, density of 0.785 g/ml, viscosity of 1.66 mPas, and relative permittivity 17.9. The reason for utilising pure fluids of low surface tension instead of surfactant solutions is to exclude surface tension gradients due to the non-uniform distribution of surfactant molecules under a focused electric. The liquid is injected at a constant flow rate of 1 ml/h in all experiments.

Polymeric and curcumin-incorporated particles generation

Polyvinylidene Fluoride (PVDF) (Sigma-Aldrich) with a molecular weight of 534000, received in the form of powder, was used to prepare the polymeric electrospray solution. The solution was mixed by dissolving PVDF in a mixture of Dimethylformamide (DMF) (Sigma-Aldrich) and Acetone (Sigma-Aldrich) in a weight ratio of 7–3 to create a 5% weight ratio PVDF solution. The solution was then electrosprayed directly inside an enclosed chamber to prevent any external airflow, using the same configuration as above. Aluminium foil for particle collection was prepared by rinsing with cleaning IPA to remove any unwanted particles. The collecting substrate was then placed inside the chamber at a distance of 8 cm from the nozzle to collect particles in 3 minutes. The substrate was then examined under the scanning electron microscope (SEM) (Thermo Fisher Scientific) with built-in energy dispersive spectroscopy (EDS) for particle imaging and elemental analysis. After collecting particles, the generated plume of particles was analysed with the optical particle sizer (TSI) and the electrometer (TSI) for size distribution and charge data. The experiment schematic for polymeric particle generation is shown in Figure. S1.

Polyvinyl alcohol (PVA) (Sigma-Aldrich) mixed with de-ionised water to prepare the 1% weight ratio PVA solution. Poly (lactic-co-glycolic acid) (PLGA) (Sigma-Aldrich) powder was mixed with acetone (Sigma-Aldrich) to create the 5% weight ratio PLGA solution. The two solutions are electrosprayed via IFENE and collected on Nylon6 filters (PALL corporation) and coated with gold before imaging with SEM.

Experiment with curcumin-incorporated particles using curcumin (Sigma-Aldrich) in powder form for solution mixing. The solution is mixed by dissolving PVDF (5% weight ratio) and curcumin (5% weight ratio) in DMF and acetone. The solution was then electrosprayed and the resulting particles were analysed with the same procedure.

Encapsulation efficiency and loading capacity

Encapsulation efficiency (EE) and loading capacity (LC) were determined by suspending the PVDF and PVDF plus curcumin particles separately in 55 ml ethanol at 25°C, 120 rpm for 1 h, thrice. The concentration of the curcumin in the supernatant was determined using BioTek Synergy H1 Hybrid Microplate reader (Bio-Tek Instruments Inc.) and a standard curve of known curcumin concentrations in ethanol by measuring absorbance at a wavelength of 425 nm [65,66]. The EE and LC percentage were calculated using the formula as follows:

$$EE = \frac{Weight\ of\ curcumin\ in\ particles}{Weight\ of\ curcumin\ in\ preparation\ solution} \times 100\%$$

$$LC = \frac{Weight\ of\ curcumin\ in\ particles}{Weight\ of\ (PVDF - curcumin)\ particles} \times 100\%$$

In vitro release

PVDF particles and PVDF-curcumin particles and free curcumin were suspended or dissolved separately in the release media (1% v/v of Tween 80 in phosphate buffer solution (PBS, pH 7.4)) [65] at 37°C and 60 rpm in an orbital shaker [66]. At predetermined time intervals of 30 min, 1, 2, 4, 6, 8, 12, 24, 36, 48 and 72 h, 1 ml of sample from PVDF and PVDF plus curcumin and 500 μl from free curcumin was withdrawn and replaced with fresh release media. The concentration of the released curcumin was determined using BioTek Synergy H1 Hybrid Microplate reader (Bio-Tek Instruments Inc.) and a standard curve of known curcumin concentrations in the release media by measuring absorbance at a wavelength 425 nm.

CRediT authorship contribution statement

Hoai-Duc Vu: Conceptualization, Formal analysis, Investigation, Methodology, Visualization, Writing – original draft. **Trung-Hieu Vu:** Investigation, Visualization. **Ngoc Luan Mai:** Formal analysis, Investigation. **Deeptee Chandrashekhar Pande:** Formal analysis, Investigation. **Dzung Viet Dao:** Supervision, Conceptualization. **Bernd H.A. Rehm:** Resources, Writing – review & editing. **Nam-Trung Nguyen:** Resources, Writing – review & editing. **Gary D. Grant:** Conceptualization, Writing – review & editing. **Canh-Dung Tran:** Writing – review & editing. **Yong Zhu:** Supervision, Writing – review & editing. **Van Thanh Dau:** Conceptualization, Funding acquisition, Methodology, Project administration, Supervision, Writing – review & editing.

Declaration of Competing Interest

The authors declare the following financial interests/personal relationships which may be considered as potential competing interests: Van Thanh Dau, Dzung Viet Dao has patent pending to Griffith University.

Data availability

Data will be made available on request.

Acknowledgement

The authors would like to express their sincere gratitude to all individuals that contributed to the successful completion of this research. We extend our heartfelt appreciation to Ms. T.V. Anh Hoang for providing invaluable insights and assistance. We are thankful for the support of Mr. T. Dung Nguyen, Mr. Dang Tran, Dr. Hung Nguyen in data collection process. Special thanks to the technical staffs at School of Engineering and Built Environment and Health Sciences in Griffith University. Additionally, the authors acknowledge Griffith University

for granting access to essential resources and facilities. Finally, we would like to acknowledge the reviewers for their constructive feedback and suggestions, which significantly improved the quality of this manuscript.

Appendix A. Supporting information

Supplementary data associated with this article can be found in the online version at doi:10.1016/j.nantod.2024.102217.

References

[1] M. Nikolaou, C.T. Krasia, Electrohydrodynamic methods for the development of pulmonary drug delivery systems, Eur. J. Pharm. Sci. 113 (2018) 29–40.
[2] A. Pawar, S. Thakkar, M. Misra, A bird's eye view of nanoparticles prepared by electrospraying: advancements in drug delivery field, J. Control. Release 286 (2018) 179–200.
[3] D.A. Groneberg, C. Witt, U. Wagner, K.F. Chung, A. Fischer, Fundamentals of pulmonary drug delivery, Respir. Med. 97 (2003) 382–387.
[4] P. Muralidharana, M. Mallorya, M. Evan, H. D.Jr. Hayes, M. Mansour, Inhalable nanoparticulate powders for respiratory delivery, Nanomedicine 11 (2015) 1189–1199.
[5] O.B. Garbuzenko, G. Mainelis, O. Taratula, T. Minko, Inhalation treatment of lung cancer: the influence of composition, size and shape of nanocarriers on their lung accumulation and retention, Cancer Biol. Med 11 (2014) 44–55.
[6] T.C. Carvalho, J.I. Peters, R.O. Williams III, Influence of particle size on regional lung deposition–what evidence is there? Int J. Pharm. 406 (2011) 1–10.
[7] F. Gagnadoux, J. Hureaux, L. Vecellio, T. Urban, A. Le Pape, I. Valo, J. Montharu, V. Leblond, M. Boisdron-Celle, S. Lerondel, C. Majoral, P. Diot, J.L. Racineux, E. Lemarie, Aerosolized chemotherapy, J. Aerosol Med Pulm. Drug Deliv. 21 (2008) 61–70.
[8] P.J. Thompson, Drug delivery to the small airways, Am. J. Respir. Crit. Care Med 157 (1998) 10–13.
[9] P.G.A. Rogueda, D. Traini, The nanoscale in pulmonary delivery. Part 1: deposition, fate, toxicology and effects, Expert Opin. Drug Deliv. 4 (2007) 595–606.
[10] P. Zanen, L.T. Go, J.W.J. Lammers, Optimal particle size for beta 2 agonist and anticholinergic aerosols in patients with severe airflow obstruction, Thorax 51 (1996) 977–980.
[11] S.P. Newman, M.A. Johnson, S.W. Clarke, Effect of particle size of bronchodilator aerosols on lung distribution and pulmonary function in patients with chronic asthma, Thorax 43 (1988) 159.
[12] L. Yue, X. Zhang, C. Zhao, R. Chen, C. Xiaoyuan, R. Lang, Inhaled drug delivery: Past, present, and future, Nano Today 52 (2023) 101942.
[13] H. Yamamoto, Y. Kuno, S. Sugimoto, H. Takeuchi, Y. Kawashima, Surface-modified PLGA nanosphere with chitosan improved pulmonary delivery of calcitonin by mucoadhesion and opening of the intercellular tight junctions, J. Control. Release 102 (2005) 373–381.
[14] Q. Liu, J. Guan, L. Qin, X. Zhang, S. Mao, Physicochemical properties affecting the fate of nanoparticles in pulmonary drug delivery, Drug Discov. Today 25 (2020) 150–159.
[15] B.Y. Shekunov, P. Chattopadhyay, H.H.Y. Tong, A.H.L. Chow, Particle size analysis in pharmaceutics: principles, methods and applications, Pharm. Res 24 (2007) 203–227.
[16] L. Cao, J. Luo, K. Tu, L.Q. Wang, H. Jiang, Generation of nano-sized core-shell particles using a coaxial tri-capillary electrospray-template removal method, Colloids Surf. B Biointerfaces 115 (2014) 212–218.
[17] J. Chen, Y. Cui, X. Xu, L.Q. Wang, Direct and effective preparation of core-shell PCL/PEG nanoparticles based on shell insertion strategy by using coaxial electrospray, Colloids Surf. A Physicochem Eng. Asp. 547 (2018) 1–7.
[18] A.S. Reddy, B.A. Lakshmi, S. Kim, J. Kim, Synthesis and characterization of acetyl curcumin-loaded core/shell liposome nanoparticles via an electrospray process for drug delivery, and theranostic applications, Eur. J. Pharm. Biopharm. 142 (2019) 518–530.
[19] W. Kim, S.S. Kim, Ag(x)VOPO(4): a demonstration of the dependence of battery-related electrochemical properties of silver vanadium phosphorous oxides on Ag / V ratios, Polymers 52 (2011) 3325–3336.
[20] F. Mou, C. Chen, J. Guan, D.R. Chen, H. Jing, Oppositely charged twin-head electrospray: a general strategy for building Janus particles with controlled structures, Nanoscale 5 (2013) 2055–2064.
[21] D. Huang, J. Wang, M. Nie, G. Chen, Y. Zhao, Adv. Mater. 35 (2023).
[22] S.A. Hofstadler, K.A. Sannes-Lowery, Applications of ESI-MS in drug discovery: interrogation of noncovalent complexes, Nat. Rev. Drug Discov. 5 (2006) 585–595.
[23] M. Wleklinski, B.P. Loren, C.R. Ferreira, Z. Jaman, L. Avramova, T.J.P. Sobreira, D. H. Thompson, R.G. Cooks, High throughput reaction screening using desorption electrospray ionization mass spectrometry, Chem. Sci. 9 (2018) 1647–1653.
[24] V.T. Dau, T.X. Dinh, C.D. Tran, T. Terebessy, T.C. Duc, T.T. Bui, Particle precipitation by bipolar corona discharge ion winds, J. Aerosol Sci. 124 (2018) 83–94.
[25] Q.T. Zhou, P. Tang, S.S.Y. Leung, J.G.Y. Chan, H.K. Chan, Emerging inhalation aerosol devices and strategies: where are we headed? Adv. Drug Deliv. Rev. 75 (2014) 3–17.
[26] M.B. Dolovich, R. Dhand, Aerosol drug delivery: developments in device design and clinical use, Lancet 377 (2011) 1032–1045.
[27] J.-W. Yoo, D.J. Irvine, D.E. Discher, S. Mitragotr, Bio-inspired, bioengineered and biomimetic drug delivery carriers, Nat. Rev. Drug Discov. 10 (2011) 521–535.
[28] A. Jaworek, A.T. Sobczyk, A. Krupa, Electrospray application to powder production and surface coating, J. Aerosol Sci. 125 (2018) 57–92.
[29] G.M.H. Meesters, P.H.W. Vercoulen, J.C.M. Marijnissen, B. Scarlett, Generation of micron-sized droplets from the Taylor cone, J. Aerosol Sci. 23 (1992) 37–49.
[30] J. Fernandez de la Mora, C. Barrios-Collado, A bipolar electrospray source of singly charged salt clusters of precisely controlled composition, Aerosol Sci. Technol. 51 (2017) 778–786.
[31] J.P. Borra, D. Camelot, K.L. Chou, P.J. Kooyman, J.C.M. Marijnissen, B. Scarlett, Bipolar coagulation for powder production: micro-mixing inside droplets, J. Aerosol Sci. 30 (1999) 945–958.
[32] J.P. Borra, D. Camelot, J.C.M. Marijnissen, B. Scarlett, A new production process of powders with defined properties by electrohydrodynamic atomization of liquids and post-production electrical mixing, J. Electrostat. 40–41 (1997) 633–638.
[33] V.T. Dau, T. Terebessy, Electrostatic Spraying Apparatus, and Current Control Method for Electrostatic Spraying Apparatus, US patent No. US9937508, 2014.
[34] L.Y. Yeo, D. Lastochkin, S.C. Wang, H.C. Chang, A new AC electrospray mechanism by maxwell-wagner polarization and capillary resonance, Phys. Rev. Lett. 92 (2004) 2–5.
[35] P. Wang, S. Maheshwari, H.C. Chang, Phys. Rev. Lett. 96 (2006) 3–6.
[36] D.B. Bober, C.-H. Chen, Pulsating electrohydrodynamic cone-jets: from choked jet to oscillating cone, J. Fluid Mech. 689 (2011) 552–563.
[37] V.T. Dau, T.K. Nguyen, D.V. Dao, Charge reduced nanoparticles by sub-kHz ac electrohydrodynamic atomization toward drug delivery applications, Appl. Phys. Lett. 116 (2020).
[38] T.-H. Vu, S. Yadav, C.-D. Tran, H.-Q. Nguyen, T.-H. Nguyen, T. Nguyen, T.-K. Nguyen, J.W. Fastier-Wooller, T. Dinh, H.-P. Phan, H.T. Ta, N.-T. Nguyen, D. V. Dao, V.T. Dau, Charge-reduced particles via self-propelled electrohydrodynamic atomization for drug delivery applications, ACS Appl. Mater. Interfaces 15 (2023) 29777–29788.
[39] V.T. Dau, T.H. Vu, C.D. Tran, T.V. Nguyen, T.K. Nguyen, T. Dinh, H.P. Phan, K. Shimizu, N.T. Nguyen, D.V. Dao, Electrospray propelled by ionic wind in a bipolar system for direct delivery of charge reduced nanoparticles, Appl. Phys. Express 14 (2021) 055001.
[40] J.R. Melcher, G.I. Taylor, Electrohydrodynamics: a review of the role of interfacial shear stresses, Annu Rev. Fluid Mech. 1 (1969) 111–146.
[41] J.U. Brackbill, D.B. Kothe, C. Zemach, A continuum method for modeling surface tension, J. Comput. Phys. 100 (1992) 335–354.
[42] C.W. Hirt, B.D. Nichols, Volume of fluid (VOF) method for the dynamics of free boundaries, J. Comput. Phys. 39 (1981) 201–225.
[43] H. Huh, R.E. Wirz, Simulation of electrospray emission processes for low to moderate conductivity liquids, Phys. Fluids 34 (2022) 1–17.
[44] G. Tomar, D. Gerlach, G. Biswas, N. Alleborn, A. Sharma, F. Durst, S.W.J. Welch, A. Delgado, Two-phase electrohydrodynamic simulations using a volume-of-fluid approach, J. Comput. Phys. 227 (2007) 1267–1285.
[45] J.R. Melcher, Continuum Electromechanics, MIT Press, Cambridge, MA, 1981.
[46] C.H. Park, J. Lee, [Performance evaluation of the Piccolo xpress Point-of-care Chemistry Analyzer], J. Appl. Polym. Sci. 114 (2009) 430–437.
[47] W.D. Ristenpart, J.C. Bird, A. Belmonte, F. Dollar, H.A. Stone, Non-coalescence of oppositely charged drops, Nature 461 (2009) 377–380.
[48] J. Wang, B. Wang, H. Qiu, Magnetic structure and magnetic transport properties of graphene nanoribbons with sawtooth zigzag edges, Sci. Rep. 4 (2014) 7587.
[49] L.N. Mai, T.H. Vu, T.X. Dinh, H.D. Vu, C.-D. Tran, V.T. Dau, H.K. Ngo, Phys. Fluids 35 (2023).
[50] Z. Liang, R. Ni, J. Zhou, S. Mao, Recent advances in controlled pulmonary drug delivery, Drug Discov. Today 20 (2015) 380–389.
[51] P.C.L. Kwok, S.J. Trietsch, M. Kumon, H.K. Chan, Electrostatic charge characteristics of jet nebulized aerosols, J. Aerosol Med Pulm. Drug Deliv. 23 (2010) 149–159.
[52] W. Glover, H.K. Chan, Electrostatic charge characterization of pharmaceutical aerosols using electrical low-pressure impaction (ELPI, J. Aerosol Sci. 35 (2004) 755–764.
[53] P.R. Byron, J. Peart, J.N. Staniforth, Aerosol electrostatics. I: Properties of fine powders before and after aerosolization by dry powder inhalers, Pharm. Res. 14 (6) (1997) 698–705.
[54] P.C.L. Kwok, H.K. Chan, Effect of relative humidity on the electrostatic charge properties of dry powder inhaler aerosols, Pharm. Res 25 (2008) 277–288.
[55] S. Hoe, D. Traini, H.K. Chan, P.M. Young, Measuring charge and mass distributions in dry powder inhalers using the electrical Next Generation Impactor (eNGI), Eur. J. Pharm. Sci. 38 (2009) 88–94.
[56] J.T. Huckaby, S.K. Lai, PEGylation for enhancing nanoparticle diffusion in mucus, Adv. Drug Deliv. Rev. 124 (2018) 125–139.
[57] J. Sharifi-Rad, Y. El Rayess, A.A. Rizk, C. Sadaka, R. Zgheib, W. Zam, S. Sestito, S. Rapposelli, K. Neffe-Skocińska, D. Zielińska, B. Salehi, W.N. Setzer, N.S. Dosoky, Y. Taheri, M. El Beyrouthy, M. Martorell, E.A. Ostrander, H.A.R. Suleria, W.C. Cho, A. Maroyi, N. Martins, Front. Pharmacol. 11 (2020).
[58] D. Lelli, A. Sahebkar, T.P. Johnston, C. Pedone, Curcumin use in pulmonary diseases: state of the art and future perspectives, Pharmacol. Res. 115 (2017) 133–148.
[59] H.J. Mehta, V. Patel, R.T. Sadikot, Curcumin and lung cancer–a review, Target Oncol. 9 (2014) 295–310.
[60] S. Yuan, F. Lei, Z. Liu, Q. Tong, T. Si, R.X. Xu, PLoS One 10 (2015).

[61] Z. Mai, J. Chen, T. He, Y. Hu, X. Dong, H. Zhang, W. Huang, F. Ko, W. Zhou, Electrospray biodegradable microcapsules loaded with curcumin for drug delivery systems with high bioactivity, RSC Adv. 7 (2017) 1724–1734.
[62] Y. Wang, X. Yang, W. Liu, F. Zhang, Q. Cai, X. Deng, Controlled release behaviour of protein-loaded microparticles prepared via coaxial or emulsion electrospray, J. Micro 30 (2013) 490–497.
[63] Y.H. Lee, M.Y. Bai, D.R. Chen, Multidrug encapsulation by coaxial tri-capillary electrospray, Colloids Surf. B Biointerfaces 82 (2011) 104–110.
[64] M.J. Cózar-Bernal, M.A. Holgado, J.L. Arias, I. Muñoz-Rubio, L. Martín-Banderas, J. Álvarez-Fuentes, M. Fernández-Arévalo, Insulin-loaded PLGA microparticles: flow focusing versus double emulsion/solvent evaporation, J. Microencapsul. 28 (2011) 430–441.
[65] Y. Zheng, Y. Chen, L.W. Jin, H.Y. Ye, G. Liu, Cytotoxicity and genotoxicity in human embryonic kidney cells exposed to surface modify chitosan nanoparticles loaded with curcumin, AAPS PharmSciTech 17 (2016) 1347–1352.
[66] V. Simion, D. Stan, C.A. Constantinescu, M. Deleanu, E. Dragan, M.M. Tucureanu, A.M. Gan, E. Butoi, A. Constantin, I. Manduteanu, M. Simionescu, M. Calin, Conjugation of curcumin-loaded lipid nanoemulsions with cell-penetrating peptides increases their cellular uptake and enhances the anti-inflammatory effects in endothelial cells, J. Pharm. Pharmacol. 68 (2016) 195–207.